Supporting Information

Regulated Silica Deposition for Porosity Control and Mechanical Enhancement of Bicontinuous Particle-Stabilized Emulsions

Meyer T. Alting[1], *Martin F. Haase*[1*]

[1] Van 't Hoff Laboratory for Physical and Colloid Chemistry, Department of Chemistry, Debye Institute for Nanomaterials Science, Utrecht University, Utrecht, The Netherlands

* Correspondence: m.f.haase@uu.nl

This PDF file included:

Supporting Information S1 **Feasibility of reinforcing bijels with TEOS**

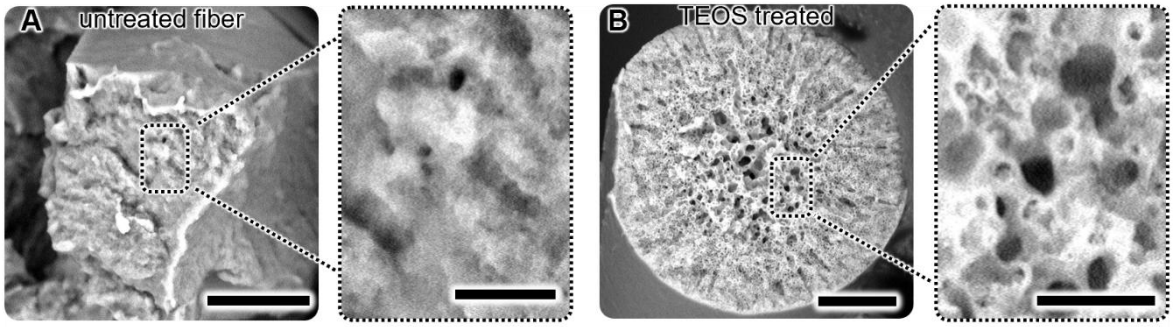

Figure S1: Dried bijel structures **A)** without and **B)** with TEOS treatment of 3 vol-% in mineral oil for 24 h, scale bar = 20 µm, in magnified image 5 µm. While the internal structure collapses upon drying for an untreated bijel, the structure remains open and porous, retaining the interwoven structure.

Supporting Information S2 **SEM images of fibers treated with 0.03 vol-% TEOS/TPOS**

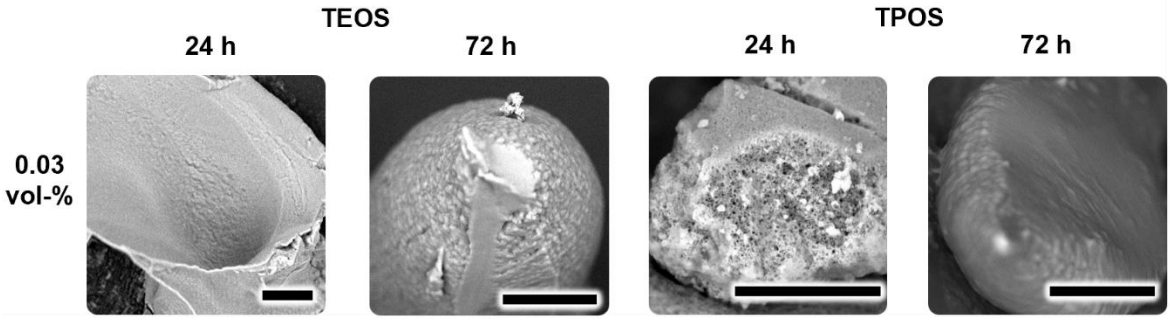

Figure S2: SEM of fibers after 24/72 h with 0.03 vol-% TEOS/TPOS in water-enriched mineral oil.

Supporting Information S3 **Volumetric change of bijel fiber during TEOS treatment**

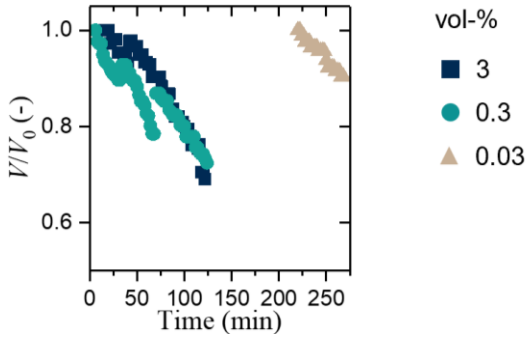

Figure S3: $V\ /\ V_0$ over time for bijel fibers during TEOS treatment with variable concentrations in water-enriched *iso*-dodecane. No distinction between 3 and 0.3 vol-% TEOS as pronounced for TPOS is visible. We expect that some reinforcement already occurred during TEOS treatment. Hence, dissolution of aqueous phase does not solely cause fiber to shrink, but is probably limited due to silica deposition. For 0.03 vol-%, no data collected before 200 min as bicontinuity preserved in this time.

Supporting Information S4 **Oil-channel during TEOS/TPOS treatments**

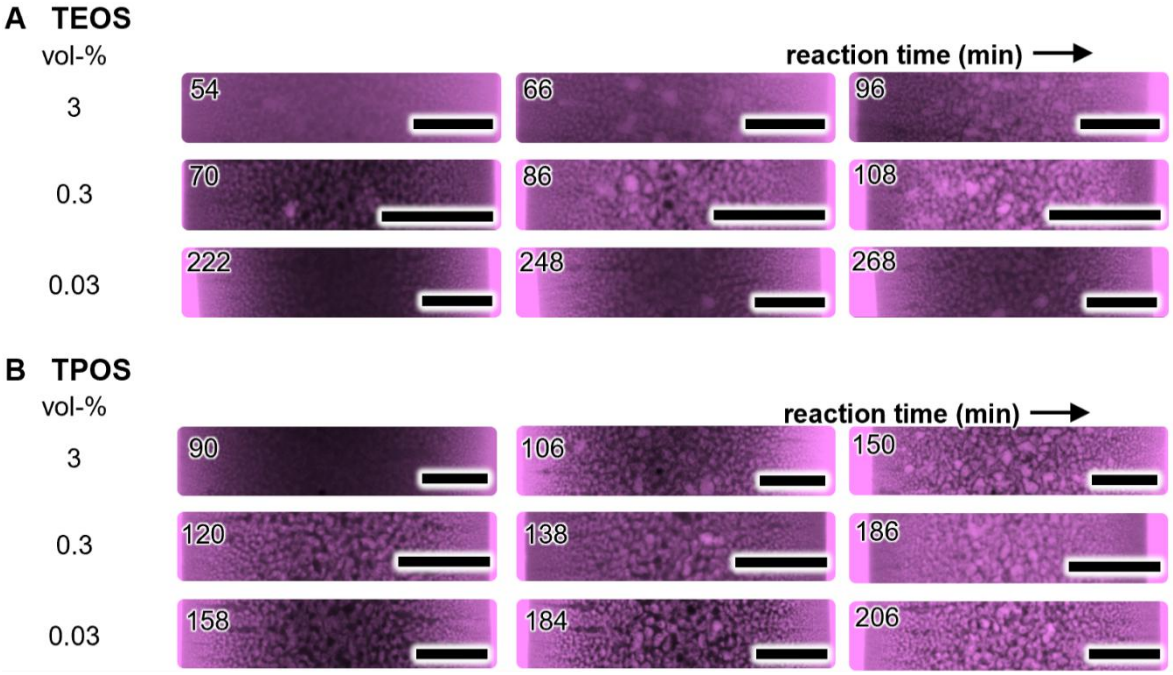

Figure S4: CLSM time series of oil-channels during TEOS and TPOS treatment in water-enriched *iso*-dodecane. Scale bar = 20 µm. Data is processed by adjusting the brightness and contrast of the micrographs. Over time, large oil voids appear in the fiber interior, appearing earlier at higher TAOS concentrations and earlier for TEOS than TPOS. The time at which these larger oil voids emerge is defined as the stability time as plotted in **Figure 3B** in the main text.

Supporting Information S5 **Contact angle of glass coverslip coated by TAOS**

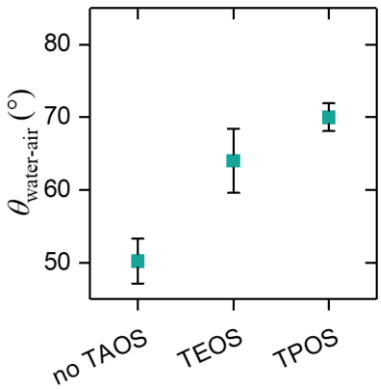

Figure S5: Contact angle of 5.0 µL water sessile droplet in water-enriched *iso*-dodecane on coverslips coated with 3 vol-% TAOS in for 6 h.

Supporting Information S6 Nile red in aqueous phase

Nile red is poorly soluble in water, leaving the aqueous phase (mixture of water at pH 2 and glycerol) in bijels non-fluorescent. During TMOS treatment, the aqueous phase becomes transient fluorescent. This effect can be reproduced by adding methanol containing Nile red to an aqueous mixture as shown in **Figure S6A**. The fluorescence is particularly enhanced in presence of glycerol. Notably, the fluorescence persists for 2 h in presence of methanol, but disappears within minutes in presence of ethanol as shown in **Figure S6B**. This effect may explain why no significant phase-coloration occurs during TEOS treatment

Interestingly, a phase-separated system of *n*-dodecane with Nile red and aqueous phase shows that methanol induces coloration of the aqueous phase from 19 vol-% on (**Figure S6C**). Emission spectra of Nile red in aqueous and *n*-dodecane phases in **Figure S6D** show strong red fluorescence around 650 nm in the aqueous phase, similar to Nile red emission adsorbed on CTAB-functionalized silica particles to detect the particle signal in CLSM images.[1,2]

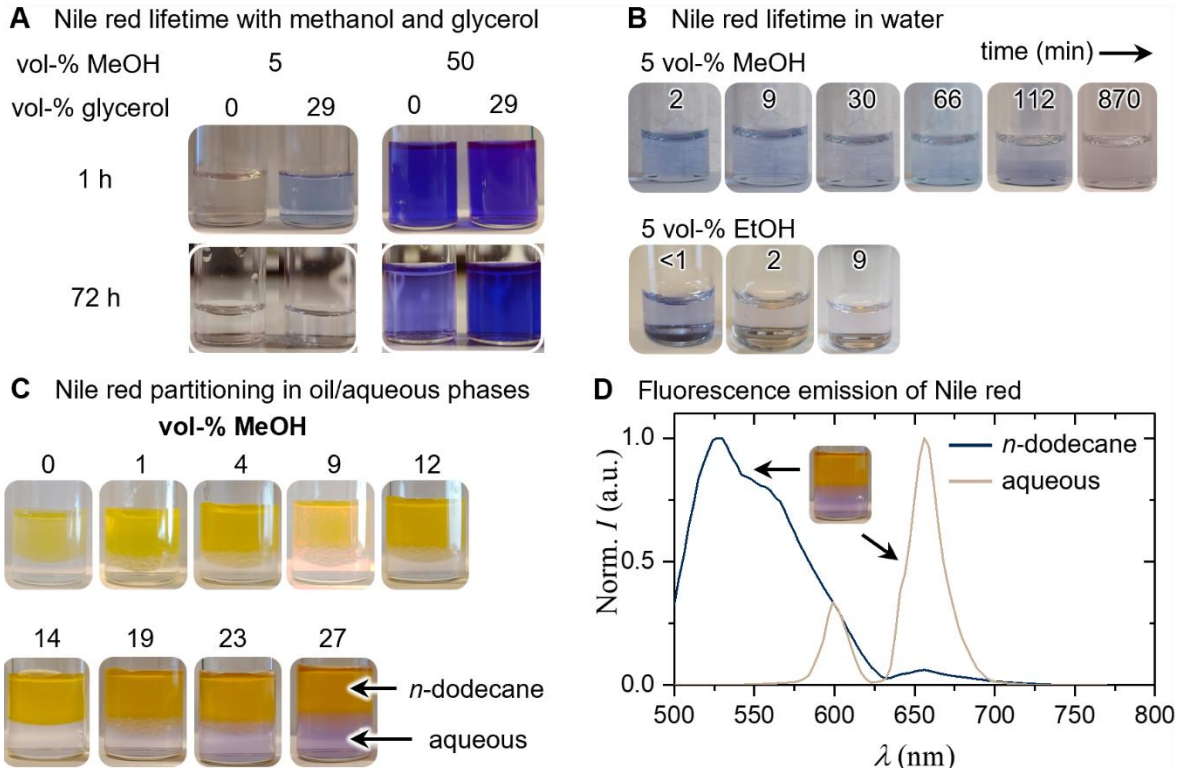

Figure S6: Nile red emission in aqueous phases. **A)** Nile red in MilliQ water pH 2.5 with variable concentrations of methanol and glycerol at times of 1 h and 72 h after mixing. **B)** Nile red added to aqueous phase containing MilliQ pH 2.5 with 29 vol-% glycerol, after which 5 vol-% of methanol containing Nile red is added. **C)** Phase separated system of (top layer) water+glycerol enriched *n*-dodecane containing Nile red and (bottom layer) aqueous phase consisting of MilliQ pH 2.5 with 29

vol-% glycerol. Then, methanol is added sequentially to increase vol-% to observe partitioning behavior of Nile red into aqueous phase. Time interval between photographs is 2 minutes.

Supporting Information S7 Oil-channel during TAOS treatment

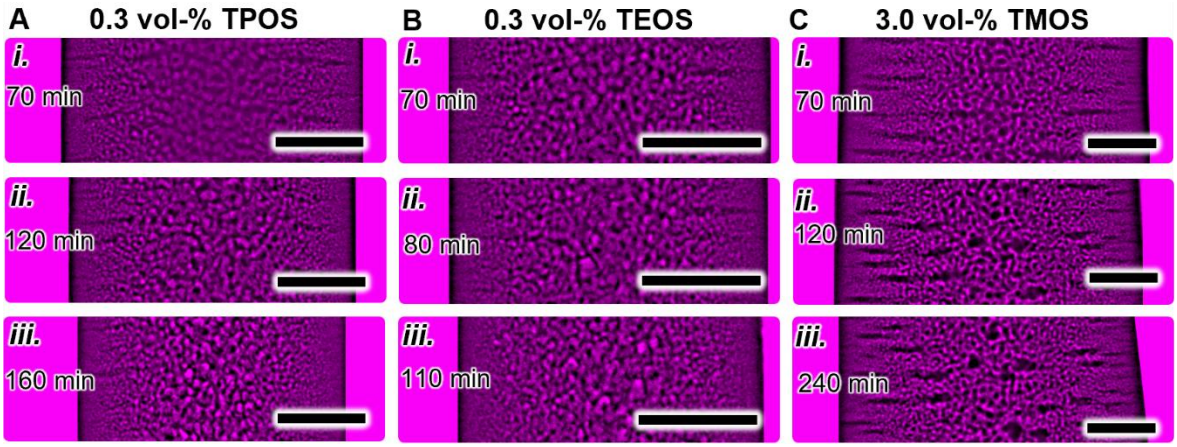

Figure S7: CLSM time series of oil-channel during TAOS treatment, composite CLSM series with particle-channel are shown in **Figures 4A**, **4B** and **4E** in main text. Scale bar = 20 µm. In these series, a bandpass filter is applied to the micrographs to improve the image resolution.

Supporting Information S8 Particle scaffold at outer fiber surface after TMOS

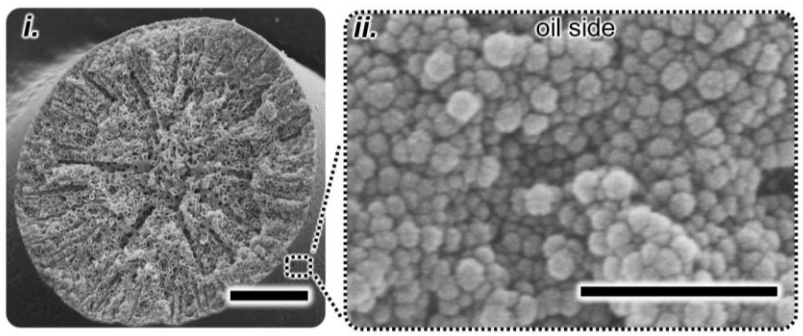

Figure S8: HR-SEM image of bijel fiber treated with 0.5 vol-% TMOS for 1.5 h as shown in **Figure 6B**. Magnifying the particle scaffold at the outer surface of the fiber in *ii*) reveals that the particles remain uncoated and spherical after TMOS-treatment. Since this surface was exposed to the surrounding oil with TMOS, this observation supports the hypothesis that hybrid silica grows directionally towards the aqueous phase. Scale bars: *i*) 20 µm and *ii*) 300 nm.

Supporting Information S9 **Effect of TAOS reaction time on reinforced bijel fiber**

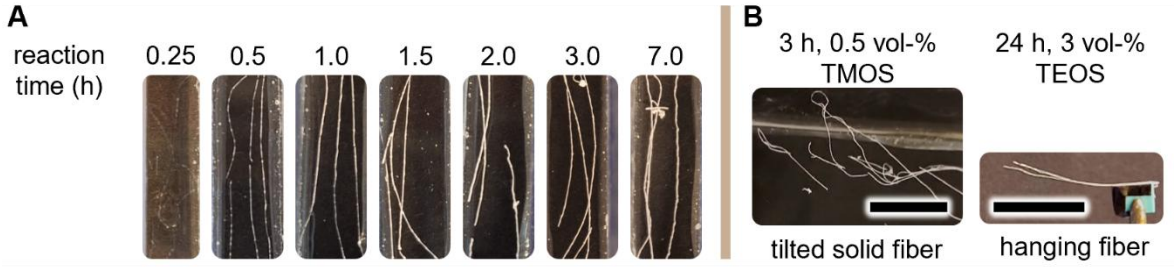

Figure S9: Dried bijel fibers treated with **A)** 0.5 vol-% TMOS with variable reaction times. An untreated bijel fiber has not been shown. **B)** Bijel fibers treated with 0.5 vol-% TMOS or 3.0 vol-% TEOS in *n*-dodecane, scale bar = 1 cm.

Supporting Information S10 **Change in oil-to-aqueous ratios for different oils**

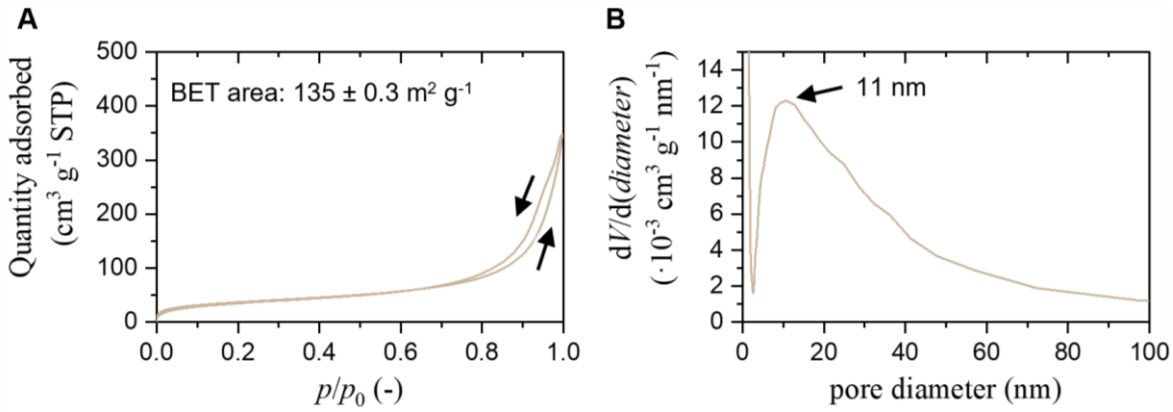

Figure S10: N_2-physisorption measurement of TEOS-treated bijel fibers. **A)** N_2 adsorption/desorption isotherm measured plotted against relative pressure p/p_0 with indication of BET specific surface area. **B)** BJH pore size distribution plotted by dV/d(*diameter*) against *pore diameter*.

Figure S10A shows the N_2-physisorption isotherm of bijel fibers treated with 3 vol-% TEOS in mineral oil for 24 h against the relative pressure p/p_0. The isotherm has a type IV shape and H1 hysteresis loop between $0.7 < p/p_0 < 1.0$.[3] These observations indicate that a mesoporous network is formed, consisting of cylindrical pores with open ends. **Figure S10B** plots the corresponding BJH pore size distribution via the differential pore volume dV/d(*diameter*) against the pore diameter,[4,5] revealing a broad peak with a maximum around 11 nm. This peak suggests that a nearly uniform mesoporous network with diameters of 11 nm are formed. Bare Ludox TMA silica nanoparticles is non-porous and does not exhibit hysteresis in the isotherm (not shown). Therefore, the observed porosity in TEOS-treated bijels is attributed to the hybrid silica deposited on the particle scaffold.

Supporting Information S11: Miscibility between alkanes and water for different types of alcohols

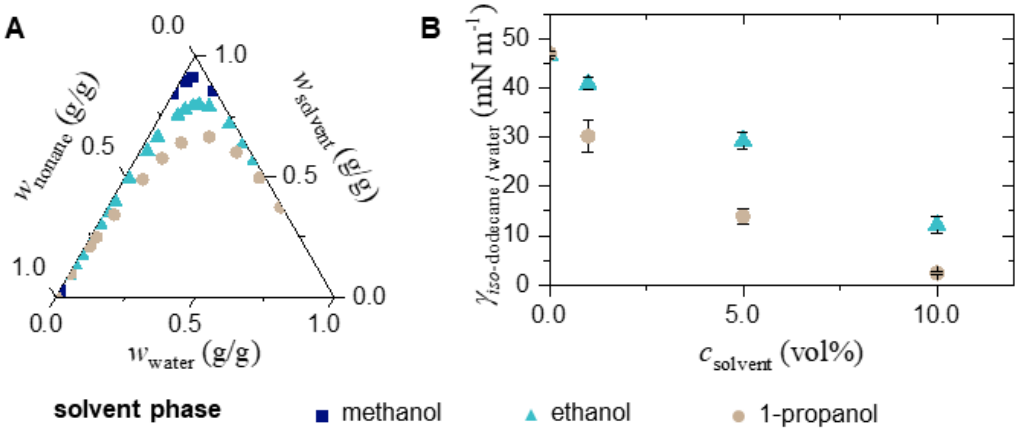

Figure S11: **A)** Ternary phase diagram of nonane, water and different solvents plotted by weight fractions w_i. Data adapted from reference [6]. **B)** Interfacial tension γ between *iso*-dodecane and water (pH 3) in presence of various concentrations of ethanol or 1-propanol. Additional details about the experiment can be found in reference [7].

The hydrolysis of TMOS, TEOS and TPOS forms methanol, ethanol and 1-propanol, respectively. The formation of these short-chain alcohols can induce miscibility between the oil- and aqueous phase in a bijel. **Figure S11A** plots a ternary phase diagram of water, nonane and these alchols.[6] Here, nonane was chosen instead of dodecane due to limited availablity of miscibility data for dodecane and methanol in the literature. However, we expect similar solubility effects for the two different alkanes due to the small difference in alkyl chain length. Figure S11A shows a downward shift of the binodal upon going from methanol to ethanol to 1-propanol, indicating a higher solubility between the oil and water phases. Additional information can be found in **Figure S11B**, where our measurements of the interfacial tension γ between *iso*-dodecane and water in presence of varying concentrations of ethanol or 1-propanol are plotted. Figure S11B shows that $\gamma_{iso-\text{dodecane/water}}$ decreases more rapidly with increasing 1-propanol concentration compared to increasing ethanol concentration. Together, these results suggest that 1-propanol can most strongly induce miscibility between the aqueous and oil phases in bijels, whereas methanol can weakly induce miscibility.

References

1 A. J. Sprockel, M. A. Khan, M. de Ruiter, M. T. Alting, K. A. Macmillan and M. F. Haase, *Colloids Surf A Physicochem Eng Asp*, 2023, **666**, 131306.

2 M. A. Khan, A. J. Sprockel, K. A. Macmillan, M. T. Alting, S. P. Kharal, S. Boakye-Ansah and M. F. Haase, *Advanced Materials*, 2022, 2109547.

3 K. S. W. Sing, D. H. Everett, R. A. W. Haul, L. Moscou, R. A. Pierotti, J. Rouquérol and T. Siemieniewska, *Pure and Applied Chemistry*, 1985, **57**, 603–619.

4 F. Rouquerol, J. Rouquerol, K. S. W. Sing, P. Llewellyn and G. Maurin, *Adsorption by Powders and Porous Solids*, Elsevier, 2014.

5 M. Thommes, K. Kaneko, A. V. Neimark, J. P. Olivier, F. Rodriguez-Reinoso, J. Rouquerol and K. S. W. Sing, *Pure and Applied Chemistry*, 2015, **87**, 1051–1069.

6 A. Skrzecz, D. G. Shaw, A. Maczynski and A. Skrzecz, *J Phys Chem Ref Data*, 1999, **28**, 983–1235.

7 H. Siegel, M. de Ruiter, T. H. R. Niepa and M. F. Haase, *J Colloid Interface Sci*, 2025, **678**, 201–208.